

Bell inequality violation in the presence of vacancies and incomplete measurements

Kaila C. S. Hall* and Daniel K. L. Oi

SUPA Department of Physics, University of Strathclyde, Glasgow, G4 0NG, United Kingdom

(Dated: December 24, 2014)

The characterization of a quantum system can be complicated by non-ideal measurement processes. In many systems, the underlying physical measurement is only sensitive to a single fixed state, complementary outcomes are inferred by non-detection leaving them vulnerable to out-of-Hilbert space errors such as particle loss. It is still possible to directly verify the violation of a Bell inequality, hence witness entanglement of a bipartite state, in the presence of large vacancy rates using such an incomplete measurement by optimizing the measurement settings. The scheme is robust against imperfect *a priori* state knowledge and also moderate amounts of error in state determination.

PACS numbers: 03.65.Ud, 03.67.-a, 03.67.Mn

I. INTRODUCTION

Non-ideal states and measurements are issues in experimental implementations of quantum information processing. Many read-out mechanisms are only sensitive to the presence of one logical state of a qubit, the complementary result is inferred from a non-detection, e.g. electron shelving in ion traps [1, 2]. Such incomplete measurements are vulnerable to vacancies or missing particles, a potential problem in schemes such as trapped particles in optical lattices where the initial state occupancy could be subject to fluctuations and where detecting the presence of a particle without disturbing its internal state is difficult [3].

Under such circumstances, it is important to be able to reliably infer important properties of the quantum system despite incomplete measurement. Here, we show how entanglement can still be detected in the presence of such imperfections by optimizing the observables measured. Even for very low occupation probability, by maximizing the classical correlation we are still able to violate the local realistic bound by exploiting the small entangled components of the mixture. The optimization is also tolerant of a small degree of measurement error, we analyze the situation corresponding to imperfect detection efficiency and dark count.

This paper is organized as follows: Sec. II describes our system and how the state is prepared depending on the vacancy position. We review the CHSH inequality in Sec. III and apply it to the situation with incomplete measurement and vacancies. We optimize the measurement settings in Sec. IV for several scenarios and finally in Sec. V we analyze the robustness of the procedure to various error models.

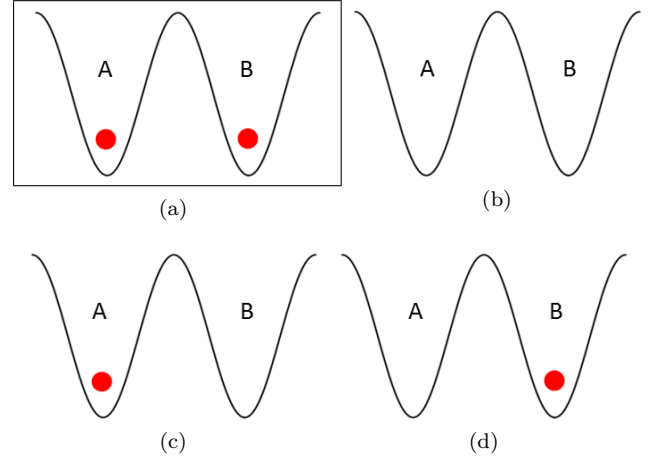


FIG. 1. (Colour online) Four possible starting states. (a) shows the entangled case, ρ_{11} , where there are two particles in the system, one in Alice's site and one in Bob's this state has probability, $(1-p)(1-q)$. (b) shows a non-entangled case, ρ_{00} , where neither Alice nor Bob have a particle in their site with probability p . In (c) is a non-entangled case where only Alice has a particle, ρ_{10} , with probability $(1-p)q\frac{1-r}{2}$. In (d) the final non-entangled case where only Bob has the particle, ρ_{01} , with probability $(1-p)q\frac{1+r}{2}$.

II. SYSTEM

We consider a bipartite system where Alice and Bob may make measurements on their respective sites as shown in Fig. 1. Ideally, they should share a joint state of two qubits but due to imperfections in state preparation one or both particles may be missing [3]. Their measurements cannot distinguish between one of the logical states or a vacant site. Despite this limitation, we are interested in whether we can still detect if there is entanglement in the system.

The local state space is spanned by the states, $\{|v\rangle, |0\rangle, |1\rangle\}$, representing a vacancy (no particle), and the logical states 0 and 1 respectively. The measurement process we consider is incomplete in the sense that it can-

* kaila.hall@strath.ac.uk

not distinguish between one of the logical states of the qubit (e.g. $|1\rangle$) or its absence, $|v\rangle$. For example, if we encode the logical states in the energy levels of an particle $\{|0\rangle = |g\rangle, |1\rangle = |e\rangle\}$, a standard readout method is to drive a cycling transition between $|g\rangle$ and third level $|f\rangle$ using a resonant laser [4]. Fluorescence is associated with a measurement outcome of the state $|0\rangle$ whereas its absence is mapped to the state $|1\rangle$, but this outcome is degenerate with the absence of the particle in the first place.

We model the situation with an initial mixed density operator with sectors corresponding to both particles missing ρ_{00} , only one particle present ρ_{01} and ρ_{10} , or both ρ_{11} . We assume there are no coherences between sectors due the lack of a suitable reference frame to lift the superselection rule on particle number [5, 6]. Hence, we can parameterize the initial state as

$$\begin{aligned} \rho_{AB}(p, q, r) &= p\rho_{00} + (1-p)\rho \\ &= p\rho_{00} \\ &+ (1-p) \left(q \left(\frac{1+r}{2}\rho_{01} + \frac{1-r}{2}\rho_{10} \right) + (1-q)\rho_{11} \right) \end{aligned} \quad (1)$$

where $\{p, q\}$ are probabilities and $-1 \leq r \leq +1$ characterizes the asymmetry in the vacancy rates of Alice and Bob. In the ideal case of no vacancy, a sequence of operations would produce the maximally entangled singlet state $|\Psi_{ideal}\rangle = \frac{1}{\sqrt{2}}(|0, 1\rangle - |1, 0\rangle)_{AB}$ as shown in Fig. 2. We assume that there is no transfer population between the two sites and that the gates are ideal. In order to detect the generation of entanglement, we may perform various measurements. As is the case in many physical systems, the physical measurement basis is fixed but preceding coherent rotations allow an arbitrary choice of basis of the state.

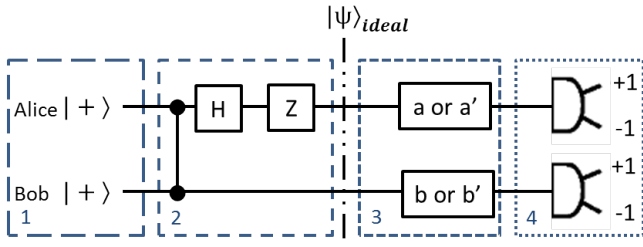


FIG. 2. (Colour online) Quantum circuit for experimental model.

- 1: Initial starting state, one of the four possible shown in Fig. 1. Here we show the ideal case where $|+\rangle = \frac{|0\rangle + |1\rangle}{\sqrt{2}}$.
- 2: Operations are performed on the particles creating the fully entangled Bell state $|\psi^-\rangle = \frac{|01\rangle - |10\rangle}{\sqrt{2}}$.
- 3: Alice (Bob) choose to measure along axis $a(b)$ or $a'(b')$ on the Bloch sphere with some probability. These measurements are performed via an active rotation of the particle.
- 4: Read out of measurement results in fixed basis.

III. DETECTING ENTANGLEMENT

A sufficient condition for a state to be entangled is that it violates a Bell inequality [7] [8]. In the simplest CHSH form this requires that Alice and Bob independently choose one of two alternative measurements $\{a, a'\}$ and $\{b, b'\}$ respectively at random and assign ± 1 to the two possible outcomes [9, 10]. Under the assumption of local realism the magnitude of the correlation function $|S| = |\langle ab \rangle + \langle ab' \rangle + \langle a'b \rangle - \langle a'b' \rangle| \leq 2$ [9]. Quantum mechanics allows $|S| = 2\sqrt{2}$ for a maximally entangled state of two qubits [11]. In our case, a vacancy adds a third possible value but due to the measurement process, it is indistinguishable from the logical state $|1\rangle$. We consider our measurement as an incomplete projection with one outcome $+1 \iff |0\rangle$ and the other degenerate, $-1 \iff |1\rangle$ or $|v\rangle$. We can represent the measurement settings a, a', b, b' as if we had a qubit but calculate the outcome probabilities to include the effect of vacancies. Hence we would like to find measurement settings that lead to a violation of local realism for a large range of vacancy probability.

A. Bound on the CHSH value

We first note that S is bounded as

$$|S| \leq \alpha 2 + (1 - \alpha) 2\sqrt{2}, \quad (2)$$

where $0 \leq \alpha \leq 1$ is the probability of having a separable state. The entangled component results in a maximum of $2\sqrt{2}$ due to the Tsirelson's bound [11] and the separable state gives a maximum of 2 for classical correlation. For any $\alpha \neq 0$ there exists the possibility of a violation of the CHSH inequality and we will see how close we can approach this bound with incomplete measurements.

B. Simplification of the CHSH Expression

The measurement settings a, a', b, b' in the ideal case of $\{p = 0, q = 0, r = 0\}$ can be written in terms of projectors and their complement on a qubit, $\cos \frac{\theta}{2} |0\rangle + e^{i\phi} \sin \frac{\theta}{2} |1\rangle$ defining a direction on the Bloch sphere where we have denoted $|0\rangle = |+\rangle$ [10]. As we model the physical measurement as a projection along a fixed axis, these settings are implemented by preceding unitary rotations that act upon the $|0\rangle, |1\rangle$ components but do not affect $|v\rangle$. Each setting is thus represented by θ and ϕ , e.g. θ_a, ϕ_a for measurement setting a . This allows an analytical express for S :

$$S = 2p + (1 - p)S', \quad (3)$$

where p is the probability of $\rho_{00}(|v, v\rangle_{AB})$ occurring, and S' is where there is at least one particle,

$$\begin{aligned}
 S' = & q \left((r-1) \cos \theta_a - (r+1) \cos \phi_b \sin \theta_b \right) \\
 & + \frac{(q-1)}{2} \left[\cos(\theta_a - \theta_b)(1 + \cos(\phi_a - \phi_b)) \right. \\
 & \quad + \cos(\theta_a + \theta_b)(1 - \cos(\phi_a - \phi_b)) \\
 & \quad + \cos(\theta_a - \theta_{b'}) (1 + \cos(\phi_a - \phi_{b'})) \\
 & \quad + \cos(\theta_a + \theta_{b'}) (1 - \cos(\phi_a - \phi_{b'})) \\
 & \quad + \cos(\theta_{a'} - \theta_b)(1 + \cos(\phi_{a'} - \phi_b)) \\
 & \quad + \cos(\theta_{a'} + \theta_b)(1 - \cos(\phi_{a'} - \phi_b)) \\
 & \quad - \cos(\theta_{a'} - \theta_{b'}) (1 + \cos(\phi_{a'} - \phi_{b'})) \\
 & \quad \left. - \cos(\theta_{a'} + \theta_{b'}) (1 - \cos(\phi_{a'} - \phi_{b'})) \right]. \quad (4)
 \end{aligned}$$

Since $|v\rangle$ always gives the result -1 , the ρ_{00} component results in the maximum classical correlation independent of the angles θ and ϕ . As long as $p < 1$ and $|S'| > 2$, then a CHSH violation is possible. Hence, for the purposes of optimization, we need only consider S' .

IV. OPTIMIZING MEASUREMENT SETTINGS

For a given state with parameters p, q and r we seek measurement setting that maximize S' ((4)), hence S . Without loss of generality, it is simple to show that it is sufficient to set $(\phi_j - \phi_k) = 0, \pi \pmod{2\pi}$ to achieve this, i.e. perform measurements only in the $X-Z$ plane. We choose $\phi_a = \phi_{a'} = \phi_b = \phi_{b'} = 0$ leading to the simplified expression

$$\begin{aligned}
 S' = & q \left((r-1) \cos \theta_a - (r+1) \sin \theta_b \right) \\
 & + (q-1) \left[\cos(\theta_a - \theta_b) + \cos(\theta_a - \theta_{b'}) \right. \\
 & \quad \left. + \cos(\theta_{a'} - \theta_b) - \cos(\theta_{a'} - \theta_{b'}) \right]. \quad (5)
 \end{aligned}$$

When Alice and Bob share a spherically symmetric singlet state ($q = 0$), S' depends only on the relative differences between the θ 's, hence it is invariant under bi-local rotations ($U_A \otimes U_B$, $U_A = U_B$) as expected. However, for ($q > 0$) the first term in Eq. (4) results in a preferred direction of measurement settings to achieve the maximum value.

A. Equal and independent vacancy rate

As an example we first consider the case where each site has an equal and independent vacancy probability P_v leading to $\rho_{AB}(P_v^2, \frac{2P_v}{(1+P_v)}, 0)$. For different values of P_v we can numerically optimize the measurement settings to maximize the value of S' and we investigate the effect of various stages of optimization (Fig. 3).

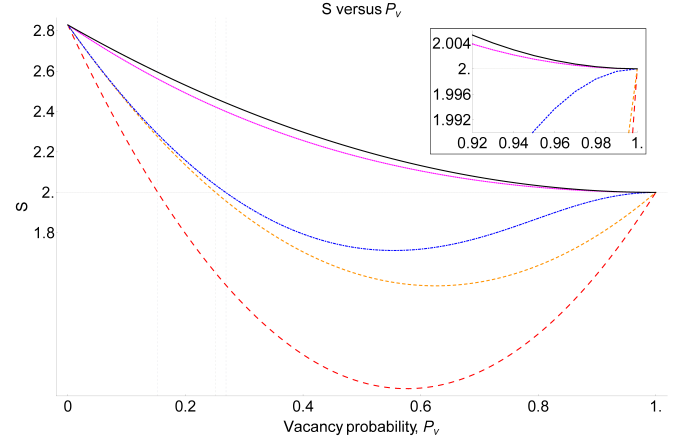


FIG. 3. (Colour online) Comparison of CHSH values for various optimizations. The black solid line is the upper bound given by Eq. (4)

No optimization (Red dashed line) Vacancy probability above which entanglement not detected $P_{v_0}^{crit} \approx 0.153$.

Step 1 (Orange dashed line) $P_{v_1}^{crit} \approx 0.251$. The optimal angle of rotation, θ is $\frac{5\pi}{8}$ for all P_v .

Step 2 (Blue dot-dashed line) $P_{v_2}^{crit} \approx 0.269$. The optimal angles of rotation for Alice and Bob's pairs of axes is different for each value of P_v .

Step 3 (Magenta dotted line) $P_{v_3}^{crit} < 1$. Again the optimal angles of rotation of each of Alice and Bob's axes are different for each value of P_v .

No Optimization: Using the conventional measurement settings (Fig. 4a) we obtain S as shown in Fig. 3 (Red dashed line). Above the critical value of $P_{v_0}^{crit} \approx 0.153$ we are unable to obtain a violation.

Step 1: We first allow a bi-local rotation around the Y axis by the same angle, i.e. redefining the global axis (Fig. 4b), this extends the critical value to $P_{v_1}^{crit} \approx 0.251$ (Fig. 3, Orange dashed line). The optimal rotation of the conventional measurement settings is $\frac{5\pi}{8}$ for all P_v which can be understood from Eq. (5), the bi-local rotation maximizes the first term but does not affect the second. As this optimization does not depend on q the optimal rotation is the same for all values of P_v .

Step 2: We rotate the the local axes independently but keep the relative angles of Alice's settings (a, a') and the relative angles of Bob's settings (b, b') the same (Fig. 4c). This leads to $P_{v_2}^{crit} \approx 0.269$ (Fig. 3, Blue dot-dashed line), however the optimal rotations are now P_v dependent.

Step 3: Finally, we optimize each measurement setting individually (Fig. 4d) [12] leading to $P_{v_3}^{crit}$ arbitrarily close to 1 (Fig. 3, Magenta dotted line). If there is some probability that there are particles in the system, then in principle we can detect at least a small amount of entanglement. Again the optimal angles of rotation are dependent upon P_v .

These optimizations progressively increase the value of P_v^{crit} to a point where we will always detect entanglement provided $P_v < 1$. In the case where $P_v \rightarrow 1$, the fully optimized measurement angles approach $\theta_a = 3.139$, $\theta_{a'} = 1.048$, $\theta_b = 4.715$ and $\theta_{b'} = 0.523$. Inserting these

into Eq. (5) we see that these measurement settings produce a value of very close to 2 for the separable part of the system and but still provides enough of a violation from the entangled component to produce a total value above 2.

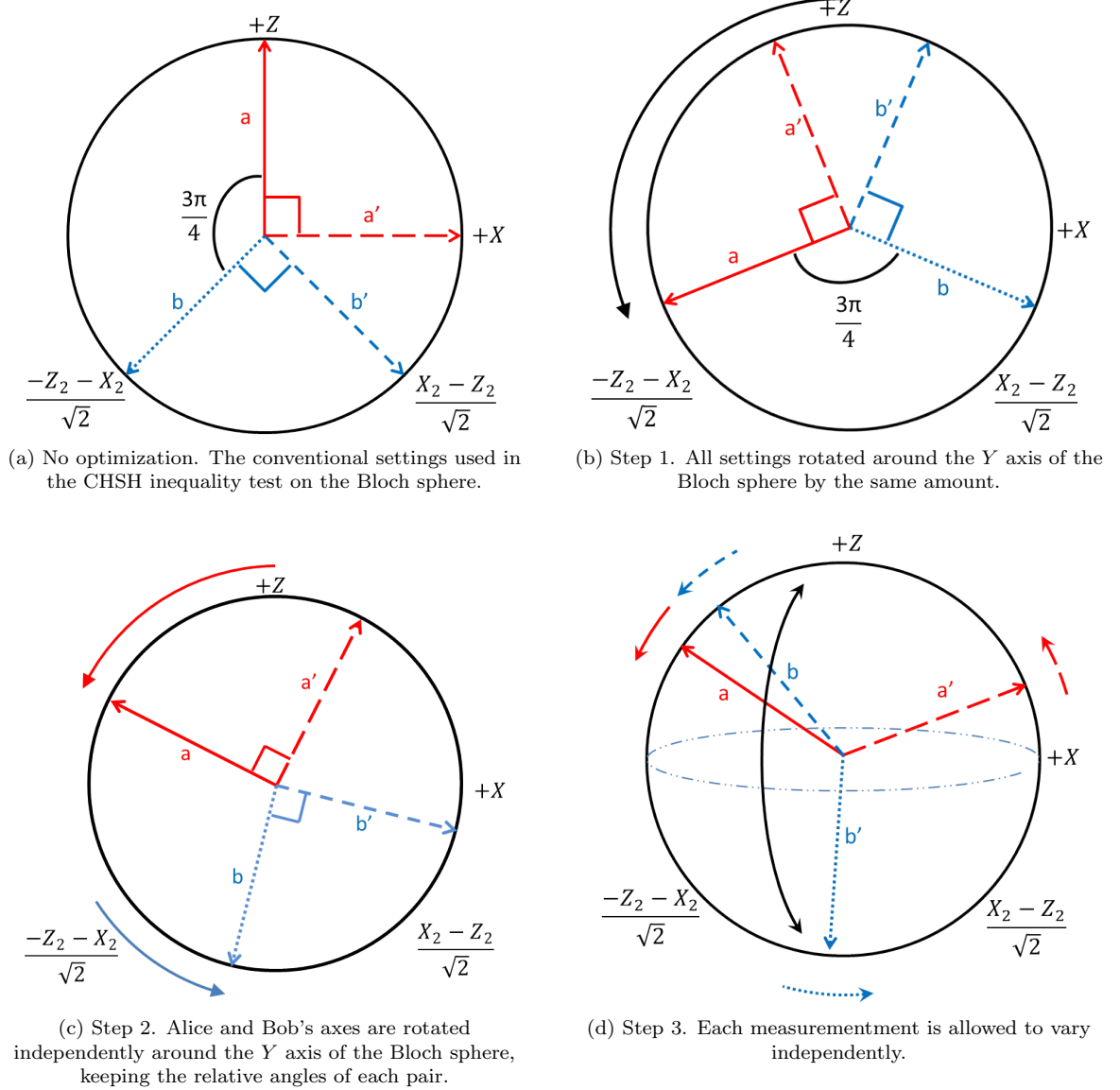


FIG. 4. (Colour online) Alice's choice of measurement settings a and a' are shown in red, Bob's choice of measurement settings b and b' in blue. These measurements are performed by an active rotation of the particle then a measurement in a fixed basis.

B. More general $\rho(p, q, r)$ states

The optimal measurement settings are not able to saturate the bound in Eq. (2) under the equal and independent vacancy rate model. This requires measurement

settings that simultaneously give 2 for the separable part and $2\sqrt{2}$ for the maximally entangled component, mirroring the right hand side of Eq. (2). We now look at more general states to see whether it can be achieved, e.g. allowing differing and correlated vacancy rates between the two sites.

Varying r (Fig. 5), which controls the symmetry in the one particle sector, we find that it is better to have a completely asymmetric system, $r = \pm 1$, to produce a larger S' . This can be understood from the description of the system $\rho(0, q, 1) = q\rho_{01} + (1 - q)\rho_{11}$, to saturate Eq. (2) we can choose settings to produce $2\sqrt{2}$ on the ρ_{11} component up to a bi-local rotation due to the spherically symmetric nature of the singlet state. Hence, this rotation can be chosen so that these measurement settings acting on ρ_{01} gives 2, the maximum correlation for a non-entangled state. In this way states with $r = \pm 1$ can saturate the bound in Eq. (2).

The dip we see as $r \rightarrow 0$ in Fig. 5 is due to the angles for the entangled and non-entangled parts no longer matching so a compromise is made between them leading to a reduced S' .

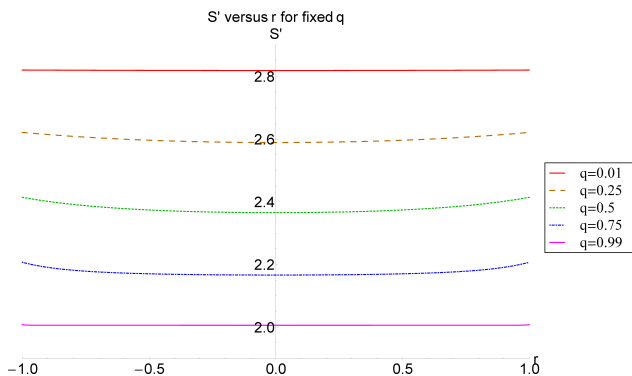


FIG. 5. (Colour online) S' versus r with a fixed q value. The optimal measurement settings for $r = -1$ are the same for all q , this is also true of $r = +1$.

V. EFFECTS OF ADDITIONAL IMPERFECTIONS

We have found that in principle we can always detect entanglement if it is present. But in experiment, additional uncertainty and noise can arise and we look at two sources of imperfections that may affect our results.

A. Robustness to state knowledge

To use most of the optimization steps in Sec. IV A it is necessary to have prior knowledge of p , q and r . In the absence of precise knowledge of these parameters, this will reduce our ability to detect a violation of the CHSH inequality. As an example, we consider the case where our estimate of q may be inaccurate. For simplicity, we will assume that our estimate of r is correct and we set $r = 0$ as this produces the smallest optimum value of S' .

We denote our uncertain estimate of the true value of q as q' . Should the true value of q be different from q' then our measurement settings will not be optimum for

q . The question becomes whether we can still detect entanglement for these non-optimum settings. Fig. 6 shows the effect of assuming different values of q' on S' . We see that it is better to be pessimistic on our estimate of q' i.e. if we choose optimum values for a higher value of q' we can detect a violation of the CHSH inequality for a larger range of q 's.

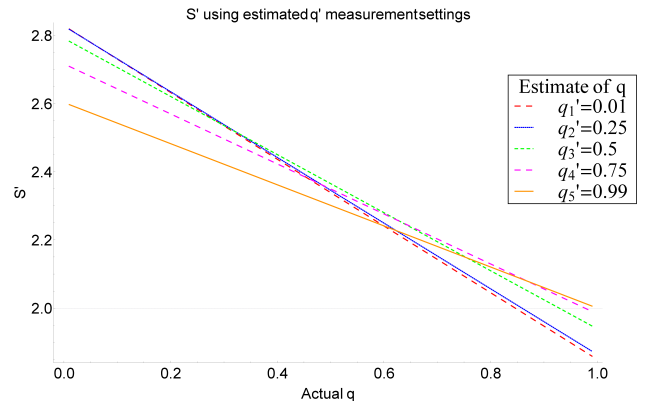


FIG. 6. (Colour online) S' for estimated q' fixed measurement settings. Using the optimal measurement settings calculated for $q'_1 \dots q'_5$ with $r = 0$ we optimize S' over the range of q individually for these five fixed measurement settings. Choosing the worst case scenario where $q' = 0.99$ (Orange solid line) shows entanglement over the whole range of q .

B. One-sided error

So far we have assumed that the detection process is 100% efficient even though it is incomplete. However real detectors can suffer from dark count and inefficiency leading to error in identifying the correct result.[13].

1. Photons/ detector inefficiency

In the case of resonance fluorescence the measurement relies on efficient capture of all the scattered photons [1, 2, 14]. Insufficient captured solid angle combined with detectors that may not register every photon that falls upon them can lead to mis-identification of the fluorescent state with the dark state or vacancy. This induces a one-sided measurement error where

$$\begin{aligned} P(+1|0\rangle) &= 1 - P(-1|0\rangle) = \eta \\ P(-1|1\rangle) &= P(-1|v\rangle) = 1 \end{aligned} \quad (6)$$

where $0 \leq (1 - \eta) \leq 1$ is the probability of incorrectly identifying the $|0\rangle$ state as $|1\rangle$ or $|v\rangle$, with the ideal case $\eta = 1$ under the model in Sec. IV A. This error does not change the measured classical correlation due to the $|v, v\rangle$ components, hence only S' needs to be considered as before.

As η decreases the CHSH violation reduces as expected (Fig. 7), however it is always possible to detect entanglement across the full range of $0 \leq P_v < 1$ when $\eta \gtrsim 0.869$. When $2(\sqrt{2} - 1) < \eta \leq 0.869$, then we obtain a violation for some values of P_v . No violation is found, even for $P_v = 0$, when $\eta \leq 2(\sqrt{2} - 1)$.

Having a sufficiently high detection efficiency is a requirement for closing the detection loophole [15–18]. For example, Garg and Mermin [17] found detector efficiency must be higher than $2(\sqrt{2} - 1)$, this value is coincidental as the assumptions and the measurement scenarios differ with our case. This is demonstrated by further optimization where the initial state (Fig. 2, Box 1) is allowed to vary as $|\psi_\tau\rangle_A |\psi_\tau\rangle_B$, $|\psi(\tau)\rangle = \cos(\tau)|0\rangle + \sin(\tau)|1\rangle$. For example, we have found states and settings that show a CHSH violation for $\eta = 0.68$ (Magenta line in Fig. 7, and Fig. 8 for no vacancies).

The measurement settings with these input states no longer sit in the $X - Z$ plane but we can specify them as a unitary rotation of the $|+Z\rangle$ direction by a rotation $[\alpha, \theta, \phi]$ where α is a rotation angle about a specified axis (θ, ϕ) in polar coordinates on the Bloch sphere. For $P_v = 0$ and $\eta = 0.68$ the optimum settings are $\tau \approx 6.11$, $a \approx [4.16, 1.95, 4.14]$, $a' \approx [2.21, 1.38, 0.77]$, $b \approx [2.83, 1.56, 1.58]$ and $b' \approx [2.46, 1.48, 0.72]$. We have not yet explored further optimization of the input state.

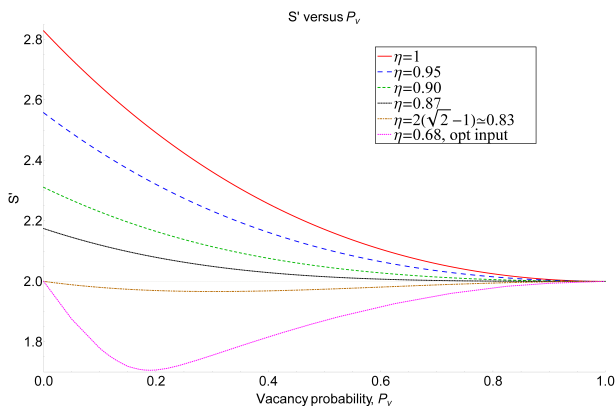


FIG. 7. (Colour online) S' value with inefficient detection. Under the model in Sec. IV A, $\eta = 0.869$ is the largest error rate that will allow the value of S to remain over 2 where $P_v < 1$, and $\eta > 2(\sqrt{2} - 1)$ is the limit that will allow a violation of the CHSH inequality for some values of P_v . By optimizing the initial input state as well, it is possible to decrease η to as low as 0.68 (Magenta line) for $P_v = 0$.

2. Error due to dark count

Dark counts can lead to the opposite one-sided error (assuming $\eta = 1$) where the dark state $|-1\rangle$ or $|v\rangle$ can

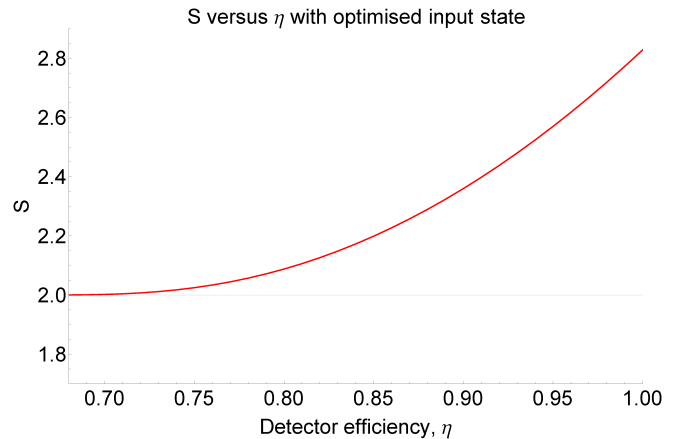


FIG. 8. (Colour online) S versus η with $P_v = 0$ for optimized input state. For $\eta = 0.68$, S just exceeds 2 hence, in principle a violation could be obtained.

be misidentified as $|0\rangle$,

$$\begin{aligned} P(+1|0) &= 1 - P(-1|0) = 1 \\ P(-1|1) &= P(-1|v) = 1 - \epsilon \end{aligned} \quad (7)$$

where $0 \leq \epsilon \leq 1$ is the error due to dark counts, with the ideal case $\epsilon = 0$ under the model in Sec. IV A [19]. From Fig. 9 we can see that if $\epsilon \geq 1 - 2(\sqrt{2} - 1)$ it is no longer possible to detect a violation of the CHSH inequality for any value of P_v . And for any $\epsilon > 0$ it is no longer possible to detect a violation of the CHSH inequality across the whole range of P_v . It is clear that the errors induced by dark count is much more destructive to the S' value.

Again, by varying the input state we can increase $\epsilon \leq 0.32$ (Fig. 9 Magenta line) and still obtain a violation for $P_v = 0$. Once again the optimized measurement settings do not sit in the $X - Z$ plane of the Bloch sphere and for $P_v = 0$ and $\epsilon = 0.32$ the optimum settings are $\tau \approx 3.31$, $a \approx [3.82, 4.18, 3.73]$, $a' \approx [4.18, 1.62, 1.95]$, $b \approx [5.95, 4.39, 1.56]$ and $b' \approx [1.45, 3.68, 4.70]$.

VI. CONCLUSION

In this paper we have explored the effects that incomplete measurement and vacancies have on the detection of entanglement using the CHSH inequality in a simple two site system. For a model with equal and independent vacancy rates, we showed that in principle it is possible to always detect a CHSH violation if entanglement is present, hence witness entanglement, by the use of optimized measurement settings. Conventional CHSH measurement settings are only able to show a violation for low vacancy rates.

As a function of the entanglement fraction of the state, we are able to saturate the bound of the CHSH value for mixtures by considering asymmetric states, ones where one side does not have any vacancies. This allows the measurement settings to simultaneously maximize the

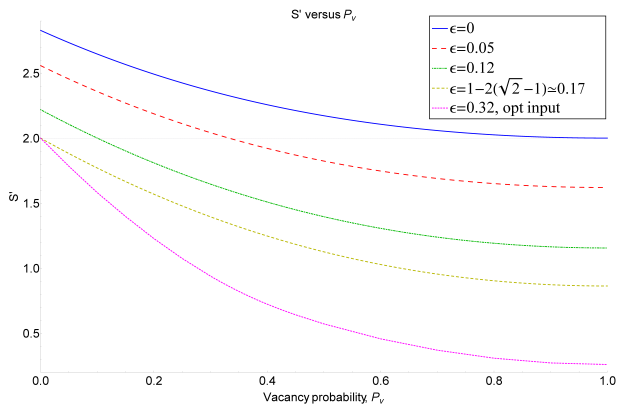


FIG. 9. (Colour online) Effect of dark count induced error on S' . When $\epsilon > 0.17$ a CHSH violation is not for any value of P_v for a $|++\rangle_{AB}$ input state. With an optimized input state the threshold for violation becomes $\epsilon \leq 0.32$, a significant improvement.

CHSH values for both the separable and maximally entangled fraction, something not possible for symmetric vacancy rates. This asymmetric system may be difficult to produce in practice or may not naturally occur, but an interesting question arises from this result, would having access to a complete local measurement that can distinguish the presence of a particle allow us to saturate the bound in Eq. (2) for more general states?

Our procedure using modified CHSH measurement settings is robust when either state knowledge or the measurement process itself are prone to error. In the case of uncertainty of the vacancy rate, a conservative estimate and associated choice of optimum settings will result in a (reduced) CHSH violation over a large range of actual vacancy rates. Choosing such optimum settings for a large vacancy rate will still allow witnessing entanglement over

most of the vacancy rate range despite uncertainty as to the actual fraction of the entangled state in the mixture.

When the measurement process is prone to a one-sided error, a CHSH violation can still be obtained for moderate levels of inaccuracy. For zero vacancy rates, the limit on the error levels for which violation can be obtained is the same for both types of one-sided error. However, in the presence of vacancies, errors due to dark count are much more detrimental to the value of the violation and considerably reduces the class of states for which entanglement can be witnessed. By optimizing the input state, the tolerable error is considerably increased. More robust states and measure settings are obtained by using initial states that do not result in a maximally entangled state in the ideal case. This trades the maximal violation on the entangled fraction for greater classical correlation on the separable part that are more resistant to the one-sided error considered here.

The precise values of detector inefficiency differ from those obtained for closing the detector loophole due to the experimental scenarios considered. In our situation, we assign a result to all experimental runs and do not discard undetected events as these are assigned the same value as the dark state. The emphasis of this work is also different, we are interested in witnessing entanglement and not necessarily closing loopholes in the violation of local-realism.

Other types of error, including those in state preparation and the implementation of the measurements rotations, will of course reduce further the class of states for which a CHSH violation (hence entanglement) can be directly witnessed. If the experimental setup has already been characterized, CHSH tests could be performed on the corrected or inferred data in order to detect entanglement though this adds a layer of complication. An analysis of more general error models will be left for future work.

-
- [1] D. J. Wineland and H. Dehmelt, *Bull. Am. Phys. Soc.* (1975).
 - [2] J. C. B. Wayne M. Itano and D. J. Wineland, *Science* **237**, 612 (1987).
 - [3] J. F. Sherson, C. Weitenberg, M. Endres, M. Cheneas, I. Bloch, and S. Kuhr, *Nature* **467**, 68 (2010).
 - [4] C. Weitenberg, M. Endres, J. F. Sherson, M. Cheneau, P. Schausz, T. Fukuhara, I. Bloch, and S. Kuhr, *Nature* **471**, 319 (2011).
 - [5] G. Wick, A. Wightman, and E. Wigner, *Phys. Rev.* **88**, 101 (1952).
 - [6] D. K. L. O. T. Paterek, P. Kurzynski and D. Kaszlikowski, *New J. Phys.* **13**, 043027 (2011).
 - [7] Of course, if one is able to perform quantum state tomography of the system, then other tests could be applied such as non-positivity of the partial transpose [20], concurrence [21, 22], etc. However, an incomplete measurement complicates the reconstruction process though strategies exist to accommodate imperfect detection [23].

- However, a Bell violation does not rely on any assumptions about the form of the measurements or the processes thus is a more direct method of verification [24].
- [8] S. M. Barnett, *Quantum Information* (Oxford University Press, New York, 2009).
- [9] J. F. Clauser, M. A. Horne, A. Shimony, and R. A. Holt, *Phys. Rev. Lett.* **23**, 880 (1969).
- [10] M. A. Nielsen and I. L. Chunag, *Quantum Computation and Quantum Information* (Cambridge University Press, 2000).
- [11] B. Tirlson, *Letters in Mathematical Physics* **4**, 93 (1980).
- [12] As previously noted, it is only necessary to optimize in the X-Z plane. Optimization over the entire Bloch sphere yields the same maximum of S' as expected.
- [13] R. H. Hadfield, *Nature Photonics* **3**, 696 (2009).
- [14] D. J. Wineland, J. C. Bergquist, W. M. Itano, and R. E. Drullinger, *Opt. Lett.* **5**, 245 (1980).
- [15] P. Pearle, *Phys. Rev. D* **2**, 1418 (1970).

- [16] T. Lo and A. Shimony, Phys. Rev. A **23**, 3003 (1981).
- [17] A. Garg and N. Mermin, Phys. Rev. D **35**, 3831 (1987).
- [18] J.-Å. Larsson, Journal of Physics A: Mathematical and Theoretical **47**, 424003 (2014).
- [19] The use of cooled detectors [25–29] should be able to reduce dark counts to negligible levels and so eliminate the effect of this error channel except for extremely high vacancy rates.
- [20] A. Peres, Phys. Rev. Lett. **77**, 1413 (1996).
- [21] W. Wootters, Phys. Rev. Lett. **80**, 2245 (1998).
- [22] S. Hill and W. Wootters, Phys. Rev. Lett. **78**, 5022 (1997).
- [23] A. F. et al., New J. Phys. **11**, 093038 (2009).
- [24] J. S. Bell, Physics **1**, 195 (1964).
- [25] R. McGrath, J. Doty, G. Lupino, G. Ricker, and J. Valterga, Electron Devices, IEEE Transactions on **34**, 2555 (1987).
- [26] W. McColgin, J. Lavine, J. Kyan, D. Nichols, and C. Stancampiano, in *Electron Devices Meeting, 1992. IEDM '92. Technical Digest., International* (1992) pp. 113–116.
- [27] W. C. McColgin, J. P. Lavine, and C. V. Stancampiano, in *Symposium B V Defect and Impurity-Engineered Semiconductors and Devices*, MRS Online Proceedings Library, Vol. 378 (1995).
- [28] W. C. McColgin, J. P. Lavine, C. V. Stancampiano, and J. B. Russell, in *Symposium D V Defect and Impurity Engineered Semiconductors and Devices II*, MRS Online Proceedings Library, Vol. 510 (1998).
- [29] R. Widenhorn, M. M. Blouke, A. Weber, A. Rest, and E. Bodegom, in *Sensors and Camera Systems for Scientific, Industrial, and Digital Photography Applications III*, Vol. 4669 (2002) pp. 193–201.